

Article

Not peer-reviewed version

STAT3 Inhibitory Activities of Lignans Isolated from the Stems of *Lindera obtusiloba* Blume

[Eun-Jae Park](#), Hee Ju Lim, [Hyung Jin Lim](#), Bong-Sik Yun, Soyoung Lee, [Seung-Jae Lee](#), [Seung Woong Lee](#)*

Posted Date: 24 October 2023

doi: 10.20944/preprints202310.1509.v1

Keywords: Lindera Obtusiloba Blume; Lignan; IL-6; JAK2; STAT3



Preprints.org is a free multidiscipline platform providing preprint service that is dedicated to making early versions of research outputs permanently available and citable. Preprints posted at Preprints.org appear in Web of Science, Crossref, Google Scholar, Scilit, Europe PMC.

Copyright: This is an open access article distributed under the Creative Commons Attribution License which permits unrestricted use, distribution, and reproduction in any medium, provided the original work is properly cited.

Article

STAT3 Inhibitory Activities of Lignans Isolated from the Stems of *Lindera obtusiloba* Blume

Eun-Jae Park ^{1,2}, Hee-Ju Lim ^{1,2}, Hyung-Jin Lim ¹, Bong-Sik Yun ², Soyoung Lee ¹,
Seung-Jae Lee ¹ and Seung Woong Lee ^{1,*}

¹ Functionality Biomaterial Research Center, Korea Research Institute of Bioscience and Biotechnology, Jeonbuk 56212, Republic of Korea

² Division of Biotechnology and Advanced Institute of Environment and Bioscience, College of Environmental and Bioresource Sciences, Jeonbuk National University, Iksan-si, Republic of Korea

* Correspondence: lswdoc@kribb.re.kr

Abstract: *Lindera obtusiloba* Blume has several activities, such as anti-inflammatory, anti-allergic, anti-tumor, anti-wrinkle, and antioxidant activities. Interleukin-6 (IL-6) is a classic pro-inflammatory cytokine that is associated with various functions, such as proliferation, invasion, inflammatory responses and functions within antioxidant defence systems. In this study, we investigated IL-6-induced STAT3 activation of lignan compounds isolated from *L. obtusiloba*. The structures of the isolated compounds were elucidated via spectroscopic nuclear magnetic resonance (NMR) and electrospray ionization mass spectrometry (ESI-MS). As a result, seven lignans were identified from *L. obtusiloba*. All the isolated compounds (**1-7**) were evaluated for their IL-6-induced STAT3 inhibitory effects in Hep3B cells using a luciferase reporter assay. Of the isolates, compounds **1** and **5** showed inhibitory effects against IL-6-stimulated STAT3 activation. Furthermore, the mRNA expression levels of inflammation-related genes such as CRP, IL-1b, and SOCS3 were significantly reduced by exposure to compound **1** and **5**. The protein levels of p-STAT3, p-JAK2 in IL-6 induced U266 cells were regulated in the presence of lignans derived from *Lindera obtusiloba* by western blot assay. Based on the results, this study of *L. obtusiloba* demonstrates that the species has promise as a bioactive candidate for the treatment of IL-6-induced STAT3-related disease.

Keywords: *Lindera Obtusiloba* Blume; lignan; IL-6; JAK2; STAT3

1. Introduction

Lindera obtusiloba Blume, a flowering plant species and deciduous broad-leaved tall tree belonging to Lauraceae, is a ubiquitous tree found mainly in Korea, Japan, and China. This plant is a known medical herb traditionally used for treating fever, abdominal pain, extravasation, and inflammation, improving of blood circulation, and preventing liver damage [1,2]. Previous phytochemical studies revealed that this medicinal plant contains several secondary metabolites, such as lignans [4], neolignans, flavonoids [3], and butanolides [5]. Extracts of this plant have been reported to have anti-tumour, anti-allergy, anti-inflammatory, anti-wrinkle, antioxidant, whitening, antiplatelet, antithrombotic, vasoprotective and antihypertensive effects [4,6–10]. Previous articles showed that *L. obtusiloba* contained daucosterol, leonuriside A and 3,4-dihydroxyphenethyl glycoside from xyle [11], germacrene B, β -caryophyllene, phytol isomer and (-)- β -elemene [12], flavonoid derivatives quercitrin and hyperoside [3], essential oil such as monoterpene and sesquiterpene [12] from leaves, secoisolariciresinol [13] and lignan derivatives (+)-syringaresinol and actifolin from stem [4].

Interleukin-6 (IL-6) is a classic pro-inflammatory cytokine important in normal cell inflammatory processes [17] and not only contributes to cancer-related inflammation but also plays crucial roles in DNA damage repair, antioxidant defence systems, proliferation, invasion, metastasis, angiogenesis and metabolic remodeling [18]. IL-6 signaling is initiated by binding IL-6 to IL-6

receptor (IL-6R) complexes, which are associated with IL-6, IL-6Ra, and gp130 receptor chains, and its activation leads to the JAK-STAT and MAPK signaling pathways [19]. Further, the activation of STAT3, which forms phosphorylated dimers that can translocate into the nucleus, promotes the expression of inflammation-related gene, such as C-reactive protein (CRP). The IL-6-induced JAK2/STAT3 signaling pathway plays a positive role in inflammation and neoplasia. The phosphorylation of JAK2 and STAT3 leads to dimerization of STAT3 and translocation to the nucleus [20].

In this study, we described for chemical structure of seven lignans from the stems of *Lindera obtusiloba* Blume on the basis of spectroscopic data such as nuclear magnetic resonance (NMR) and electrospray-ionization mass spectrometry (ESI-MS) as well as evaluated for inhibitory activities on IL-6/STAT3 activation of all isolated compounds.

2. Materials and Methods

2.1. General experimental procedures

^1H , ^{13}C and 2D NMR spectra were generated using a JEOL JNM-ECA 400 and JEOL JNM-ECA600 instruments (JEOL, Tokyo, Japan) using TMS as an internal standard. Optical rotations were obtained on a Jasco P-2000 polarimeter (Jasco Corp., Tokyo, Japan). High resolution election spray ionization mass spectrometry (HRESIMS) data were acquired using a Waters SYNAPT G2-Si HDMS spectrometer (Waters, Milford, MA, USA). Column Chromatography (C.C) was performed using Silica gel (Kieselgel 60, 200 – 400 mesh, Merck, Darmstadt, Germany) and Sephadex LH-20 (GE Healthcare, Uppsala, Sweden). Each fraction was monitored by TLC profiling using silica gel 60 F₂₅₄ and RP-18 F_{254s} (Merck, Burlington, USA) and medium-pressure liquid chromatography (MPLC, CombiFlash RF, Teledyne Isco, Lincoln, NE, USA) were used to separate the fractions of the extract. semipreparative high-speed liquid chromatography (semipreparative HPLC) was conducted using a Shimadzu LC-6AD instrument (Shimadzu Corp., Tokyo, Japan) equipped with an SPD-20A detector and Phenomenex Luna C₁₈ (21.2mm × 250 mm, 5 μ m) column. All fractions and compounds were analyzed using an Agilent 1200 series HPLC system (Agilent, Santa Clara, USA).

2.2. Extraction and isolation

Dried stem of *Lindera Obtusiloba* Blume was extracted with 50% EtOH 200L at 70°C (5h, ×10). After filtering (No. 10, 600mm, Hyundai Micro Co., Seoul, South Korea), the filtrates were concentrated under reduced pressure to obtain 554.3g of extract. The residue (500 g) was suspended in distilled water (5 L), and the aqueous layer was partitioned with *n*-hexane, EtOAc and BuOH. The EtOAc layer (71.24 g) was subjected to silica gel column eluted with *n*-hexane:EtOAc (1:0 → 0:1, *v/v*), EtOAc:MeOH (9:1 → 0:1, *v/v*) to obtain 10 fractions (EA1 ~ EA10). Fraction EA5 (801.3 mg) was subjected to a Sephadex LH-20 column eluted with MeOH to yield 7 subfractions (EA5-1~7). Fraction EA5-6 (81.1 mg) was subjected to a Sephadex LH-20 column eluted with MeOH and further purified by preparative HPLC (Phenomenex Luna C₁₈ column 250 × 21.2mm, 5 μ), and isocratic elution with 50% CH₃CN in H₂O to afford compound **1** (11.1mg). Compound **4** (2.2 mg) was obtained from fraction EA5-2 (93.5 mg) by preparative HPLC (Phenomenex Luna C₁₈ column 250 × 21.2mm, 5 μ), using isocratic elution with 40% CH₃CN in H₂O. Fraction EA7 (3.27 g) was subjected to silica gel column eluted with CHCl₃:MeOH (50:1 → 0:1, *v/v*) to yield 15 subfractions (EA7-1~15). Fraction EA7-5 (152.5 mg) and Fraction EA7-8 (200.1 mg) was further purified by preparative HPLC (Phenomenex Luna C₁₈ column 250 × 21.2mm, 5 μ), and isocratic elution with 30% and 40% CH₃CN in H₂O to afford compounds **3** (4.5 mg) and **5** (5.7 mg). Compound **6** (2.7 mg) was obtained from fraction EA7-12 (104.5 mg) by preparative HPLC (Phenomenex Luna C₁₈ column 250 × 21.2mm, 5 μ), using isocratic elution with 20% CH₃CN in H₂O. Fraction EA8 (10.45 g) was subjected to MPLC [column: Silica RediSepRf (40 g); mobile phase: CHCl₃:MeOH (50:1 → 0:1, *v/v*)] to yield 20 subfractions (EA8-1~20). Fraction EA8-13 was purified by preparative HPLC (Phenomenex Luna C₁₈ column 250 × 21.2mm, 5 μ), using isocratic elution with 30% and 35% CH₃CN in H₂O to obtain compound **7** (2.2 mg) and compound **2** (4.7mg).

Episesamin (1) : white amorphous powder, ESI-MS ion peaks at m/z 358.1 [M + H]⁺, ¹H NMR data (chloroform-*d*, 500MHz): δ_H 6.84 (2H, sd, $J = 1.5$ Hz, H-2',2''), 6.79 (2H, m, $J = 8$ Hz, H-6'6''), 6.76 (2H, m, $J = 8$ Hz, H-5',5''), 4.81 (1H, d, $J = 5$ Hz, H-6), 4.37 (1H, d, $J = 7$ Hz, H-2), 4.07 (1H, d, $J = 9.5$ Hz, H-4a), 3.82 (1H, m, H-8b), 3.8 (1H, m, H-4b), 3.28 (2H, m, H-5, 8a), 2.84(1H, m, H-1), 5.94 (2H, s, O-CH₂-O), 5.92 (2H, s, O-CH₂-O); ¹³C NMR data (chloroform-*d*, 150MHz) δ_C 148.13 (C-3'), 147.81 (C-4'), 147.38 (C-4''), 146.74 (C-3''), 135.29 (C-1'), 132.43 (C-1''), 119.79 (C-6'), 118.87 (C-6''), 108.34 (C-5',5''), 106.75 (C-2'), 106.59 (C-2''), 87.84(C-2), 82.83 (C-6), 71.72 (C-4), 69.88 (C-8), 54.86 (C-1), 50.36 (C-5), 101.24 (O-CH₂-O), 101.17 (O-CH₂-O)

2-(1,3-Benzodioxol-5-yl)tetrahydro-4-[(4-hydroxy-3-methoxyphenyl)methyl]-3-furanmethanol (2) : Yellow syrup, $[\alpha]_D^{25}$ 11.23 (*c* 0.046 CH₃OH), ESI-MS ion peaks at m/z 358.1 [M + H]⁺, ¹H NMR data (methanol-*d*₄, 500MHz): δ_H 6.84 (1H, d, $J = 1.5$ Hz, H-6'), 6.79 (1H, d, $J = 2$ Hz, H-6), 6.78 (1H, d, $J = 1.5$ Hz, H-2'), 6.77 (1H, d, $J = 8$ Hz, H-3'), 6.67 (1H, d, $J = 8$ Hz, H-3), 6.63 (1H, dd, $J = 2, 8$ Hz, H-2), 4.75 (1H, d, $J = 6.5$ Hz, H-7'), 3.97 (1H, dd, $J = 6.5, 8.5$ Hz, H-9b), 3.73 (1H, dd, $J = 6, 8.5$ Hz, H-9a), 3.82 (1H, dd, $J = 7.5$ Hz, H-9'b), 3.63(1H, dd, $J = 6.5, 11$ Hz, H-9'a), 2.71 (1H, m, H-8), 2.92 (1H, dd, $J = 5, 13.5$ Hz, H-7b), 2.49 (1H, dd, $J = 11, 13.5$ Hz, H-7a), 2.33 (1H, m, H-8'), 3.83 (3H, s, OCH₃-5), 5.9 (2H, d, O-CH₂-O); ¹³C NMR data (methanol-*d*₄, 150MHz): δ_C 149.38 (C-5'), 149.13 (C-5), 148.51 (C-4'), 145.96 (C-4), 138.64 (C-1'), 133.61 (C-1), 122.28 (C-2), 120.52 (C-2'), 116.63 (C-3), 113.53 (C-6), 108.97 (C-3'), 107.4 (C-6'), 84.13 (C-7'), 73.75 (C-9), 60.57 (C-9'), 54.35 (C-8'), 44.01 (C-8), 33.75 (C-7), 56.52 (OCH₃-5), 102.44 (O-CH₂-O)

Syringaresinol (3), Light brown syrup, ESI-MS ion peaks at m/z 418.0 [M + H]⁺, ¹H NMR data (DMSO-*d*₆, 500MHz): δ_H 6.6 (4H, s, H-2',2'',6',6''), 4.61 (2H, d, $J = 3.5$ Hz, H-2,6), 4.16 (2H, dd, $J = 7, 8$ Hz, H-4,8), 3.78 (2H, dd, $J = 3.5$ Hz, H-4,8), 3.05 (2H, m, H-1,5), 3.75 (12H, s, OCH₃-3',3'',5',5''), 8.22 (2H, s, OH-4',4''); ¹³C NMR data (DMSO-*d*₆, 150MHz): δ_C 147.84 (C-5',5'',3',3''), 134.81 (C-4',4''), 131.38 (C-1',1''), 103.62 (C-2',2'',6',6''), 85.27 (C-2,6), 71.02 (C-4,8), 53.61 (C-1,5), 55.99 (OCH₃-5',5'',3',3'')

(7S,8R,8R)-lyoniresinol-9-O-(E)-feruloyl ester (4) light brown solid, $[\alpha]_D^{25}$ 3.00 (*c* 0.016 CH₃OH), LC-MS ion peaks at m/z 595 [M + H]⁺, ¹H NMR data (chloroform-*d*, 500MHz): δ_H 7.56 (1H, d, $J = 15$ Hz, H-7''), 7.04 (1H, dd, $J = 8, 2$ Hz, H-6''), 7.01 (1H, sd, $J = 2$ Hz, H-2''), 6.9 (1H, d, $J = 8$ Hz, H-5''), 6.48 (1H, s, H-2), 6.33 (2H, s, H-2, 6), 6.21 (1H, d, $J = 15$ Hz, H-8''), 4.35 (1H, d, $J = 5, 11$ Hz, H-7'), 4.29 (1H, dd, $J = 5$ Hz, 11, H-9a), 4.14 (1H, dd, $J = 6, 11$ Hz, H-9b), 3.6 (2H, m, H-9'), 2.68 (2H, m, $J = 4.5, 15$ Hz, H-7), 2.03 (1H, m, H-8'), 1.96 (1H, m, H-8), 3.92 (3''-OCH₃), 3.87 (3-OCH₃), 3.77 (3',5'-OCH₃), 3.39 (5-OCH₃), 5.83 (4''-OH), 5.33 (4'-OH), 5.31 (4-OH); ¹³C NMR data chloroform-*d*, 150MHz): δ_C 167.55 (C=O), 148.38 (C-4''), 147.03 (C-3',5'), 146.99 (C-3',5'), 146.42 (C-4), 145.86 (C-5), 145.52 (C-7''), 137.94 (C-1'), 137.31 (C-4), 133.11 (C-4'), 128.62 (C-6), 127.04 (C-1''), 125.12 (C-1), 123.44 (C-6''), 115.25 (C-8''), 114.93 (C-5''), 109.58 (C-2''), 106.25 (C-2), 105.35 (C-2,6), 67.71 (C-9), 63.82 (C-9'), 47.83 (C-8,8'), 41.7 (C-7'), 60.17 (5-OCH₃), 56.66 (3',5'-OCH₃), 56.35 (3''-OCH₃), 56.25 (3-OCH₃),

(-)-(2R,3R)-1-O-feruloyl-8,8'-bisdihydrosiringenin (5) Brown syrup, $[\alpha]_D^{25}$ 1.55 (*c* 0.024 CH₃OH), ESI-MS ion peaks at m/z 597.0 [M + H]⁺, ¹H NMR data (DMSO-*d*₆, 600MHz): δ_H 7.49 (1H, dd, $J = 16$ Hz, H-7''), 7.23 (1H, s, H-2''), 7.05 (1H, d, $J = 9$ Hz, H-6''), 6.72 (1H, d, $J = 8$ Hz, H-5''), 6.39 (1H, d, $J = 16$ Hz, H-8''), 6.35(2H, s, overlap, H-2,6,2',6'), 6.34 (2H, s, overlap, H-2,6,2',6'), 4.26 (1H, dd, $J = 5.9$ Hz, H-9a), 4 (1H, dd, $J = 5.5, 9$ Hz, H-9b), 3.51 (1H, dd, $J = 5.5, 9$ Hz, H-9'a), 3.4 (1H, dd, $J = 5.5, 9$ Hz, H-9'b), 2.7 (1H, dd, $J = 5.5, 11.5$ Hz, H-7a), 2.58 (1H, dd, $J = 5.5, 11$ Hz, H-7'a), 2.5 (2H, m, overlap, H-7b, 7'b), 2.2 (1H, m, H-8), 3.79 (3''- OCH₃), 3.67 (6H, 3,5,3',5'- OCH₃), 3.66 (6H, 3,5,3',5'- OCH₃); ¹³C NMR data (DMSO-*d*₆, 150MHz): δ_C 166.76 (C-9''), 150.59 (C-4''), 148.23 (C-3''), 147.71 (C-3,5,3',5'), 147.66 (C-3,5,3',5'), 145.04 (C-7''), 133.55 (C-4,4'), 133.38 (C-4,4'), 131.04 (C-1'), 130.37 (C-1), 124.49 (C-1''), 123.52 (C-6''), 115.56 (C-5''), 113 (C-8''), 110.95 (C-2''), 106.23 (C-2,6,2',6'), 64.45 (C-9'), 64.05 (C-9), 42.7 (C-8'), 38.51 (C-8), 34.34 (C-7), 34.1 (C-7'), 55.8 (3,5,3',5'-OCH₃), 55.75 (3,5,3',5'-OCH₃), 55.59 (3''-OCH₃)

(-)-Lyoniresinol (6) yellow syrup, $[\alpha]_D^{25}$ -7.4 (*c* 0.024 CH₃OH), ESI-MS ion peaks at m/z 419.1 [M + H]⁺, ¹H NMR data (methanol-*d*₄, 600MHz): δ_H 6.6 (1H, s, H-6), 6.4 (2H, s, H-2',6'), 4.31 (1H, d, $J = 6$ Hz, H-7'), 3.6 (1H, dd, $J = 4.8, 10.8$ Hz, H-9a), 3.5 (2H, m, overlap, H-9b, 9'), 2.7 (1H, dd, $J = 4.8, 15$ Hz, H-7a), 2.57 (1H, dd, $J = 11.4, 15$ Hz, H-7b), 1.98 (1H, m, H-8'), 1.65 (1H, m, H-8); ¹³C NMR data (methanol-*d*₄, 150MHz): δ_C 149.09 (C-3',5'), 148.77 (C-5), 147.8 (C-3), 139.93 (C-1'), 139.01 (C-4), 134.63

(C-4'), 130.29 (C-2), 126.37 (C-1), 107.88 (C-6), 106.97 (C-2',6'), 66.91 (C-9), 64.29 (C-9'), 49.18 (C-8'), 42.45 (C-7'), 41.03 (C-8), 33.72 (C-7), 60.29 (3-OCH₃), 56.89 (3', 5'-OCH₃), 56.73 (5-OCH₃)

Schizandriside (7) brown solid, $[\alpha]_D^{25}$ 12.8 (c 0.001 CH₃OH), ESI-MS ion peaks at m/z 491.0[M + H]⁺, ¹H NMR data (DMSO-*d*₆, 500MHz): δ_H 6.78 (1H, sd, *J* = 1.8 Hz, H-2), 6.68 (1H, d, *J* = 7.2 Hz, H-5), 6.6 (1H, s, H-2'), 6.48 (1H, dd, *J* = 1.8, 7.8 Hz, H-6), 6.07 (1H, s, H-5'), 4.01 (2H, sd, *J* = 11.2 Hz, H-7), 3.91 (1H, d, *J* = 7.5 Hz, H-1''), 3.83 (1H, dd, *J* = 1.8, 9.6 Hz, H-9b), 2.98 (1H, m, H-9a), 3.65 (1H, dd, *J* = 5.4, 11.4 Hz, H-5''b), 2.96 (1H, m, H-5''a), 3.57 (1H, m, H-9'b), 3.47 (1H, m, H-9'a), 3.27 (1H, overlap, H-4''), 3.08 (1H, t, *J* = 8.4 Hz, H-3''), 2.98 (1H, m, H-2''), 2.71 (2H, d, *J* = 8.1 Hz, H-7'), 1.87 (1H, m, H-8'), 1.7 (1H, t, *J* = 10.2 Hz, H-8), 3.72 (3-OCH₃), 3.7 (3'-OCH₃); ¹³C NMR data DMSO-*d*₆, 150MHz): δ_C 147.08 (C-3), 145.43 (C-3'), 144.43 (C-4), 143.99 (C-4'), 136.79 (C-1), 132.58 (C-1'), 126.97 (C-6'), 121.03 (C-6), 116.21 (C-5'), 115.4 (C-5), 113.86 (C-2), 111.81 (C-2'), 104.46 (C-1''), 76.53 (C-3''), 73.3 (C-2''), 69.53 (C-4''), 67.26 (C-9), 65.62 (C-5''), 62.62 (C-9'), 45.8 (C-7), 44.86 (C-8), 37.98 (C-8'), 31.75 (C-7'), 55.57 (C-3), 55.49 (C-3)

2.3. Cell culture

Human hepatoma Hep3B (HB-8064) cell line was obtained from the American Type Culture Collection (ATCC, Rockville, MD, USA). Hep3B cells were cultured in Dulbecco's modified Eagle's medium (DMEM, Gibco, Grand Island, NY, USA) supplemented with 10% heat-inactivated fetal bovine serum (Gibco-BRL, Cat. No. 16000-044), 50 U/mL penicillin and 100 mg/mL hygromycin (InvivoGen, Cat. No. ant-hg-1). The cells were maintained under standard cell culture conditions in an atmosphere of 5% CO₂ at 37°C.

2.4. Cell viability

The MTT (3-(4,5-dimethylthiazol-2-yl)2,5-diphenyltetrazolium bromide) assay was performed to assess of cell viability. Hep3B Cells (3 × 10⁴ cells/well) were seed in a 96-well flat-bottom microplate and incubated for 24 hours at 37°C in a CO₂ incubator. After treatment with the extracts, fractions and compounds for 24 hours, MTT solution (0.5mg/ml) was added to each well, and incubated for 3 hours. Then the supernatant was removed, and the formed formazan crystals were dissolved by adding 200µL of dimethyl sulfoxide (DMSO) per well for 30 min at 37°C in a CO₂ incubator. The absorbance measurement of each well was read at 540 nm using a microplate reader (Varioskan LUX, Thermo Fisher Scientific Inc., Waltham, MA, USA).

2.5. IL-6 induced STAT3 luciferase reporter assay.

Hep3B cells (3 × 10⁴ per well) stably transformed with pSTAT3-Luc were seed into 96-well culture plates and stabilized for 24 hours. Then the medium was replaced with serum-free medium and incubated for 12 hours. The cells were treated with extracts or compounds for 1 hour followed by stimulation with 10ng/ml IL-6. After incubation for 12 hours, the medium was removed, and Passive Lysis Buffer (Promega Corp., Madison, WI, USA) was added at 60µL/well. Then lysed for 30 min, the cells lysates (25µL) were transferred to the wells (White 96-well plate). The luciferase activity was evaluated according to the manufacturer's instructions (Promega Corp., Madison, WI, USA). The inhibitory activity with half-maximal inhibitory concentration (IC₅₀) values (means ± S.D.) were calculated from dose-response curves of six concentrations of each compound versus normalized luciferase activity in three independent experiments (*n*=3) and this value was used as a measure of the inhibitory activity. Human IL-6 and static IL-6, used for the control group, were obtained from R&D System (Minneapolis MN, USA) and Sigma-Aldrich Ltd. (St. Louis, MO, USA), respectively.

2.5.1. Real-time PCR

Real-time PCR was performed according to previously reported methods [Jang et al., 2019]. Briefly, the total cellular RNA was extracted from the Hep3B cells (1 × 10⁶ cells/well in a 6-well plate) using a Pure Link RNA Mini Kit (Invitrogen) following the manufacturer's protocol. The complementary DNA (cDNA) was synthesized from 1 µg of the total RNA using a Superscript III

First-Strand Synthesis Super Mix for qRT-PCR (Invitrogen). Quantitative real-time PCR of CRP (Hs04183452_g1), IL-1 β (Hs01555410_ma), and SOCS3 (Hs02330328_s1) was performed with a TaqMan Gene Expression Assay Kit (Applied Biosystems). To normalize the gene expression, and 18S rRNA endogenous control (Applied Biosystems) was used. Quantitative real-time PCR was employed to verify the mRNA expression using a Step-One Plus Real-Time PCR System (Applied Biosystems). cDNA (1 μ L), 0.5 μ L of the TaqMan Gene Expression Master Mix, 0.2 μ L of 18S rRNA endogenous control and 3.3 μ L of dH₂O were combined to give reaction mixtures with final volumes of 10 μ L in each reaction tube. The amplification conditions were as follows: 10s at 95°C, 60 cycles of 5s at 95°C and 30s at 60°C, 15s at 95°C, 30s at 60°C, and 15s at 95°C.

2.5.2. Western blot analysis

U266 cells were stimulated with IL-6 (10 ng/mL) for 20 min in the presence or absence of compound. Western blot analysis was conducted to assess STAT3 and JAK2 protein expression in the U266 cell line, as reported study [Lee et al., 2016]. The phosphorylation status of JAK2, STAT3, and ERK was examined using anti-phospho-STAT3 (1:1000), anti-STAT3 (1:1000), anti-phospho-JAK2 (1:1000), anti-JAK2 (1:1000), anti-phospho-ERK (1:1000), and anti-ERK (1:1000) antibodies (Cell Signaling, Beverly, MA, USA) and then were incubated with the appropriate horseradish peroxidase-conjugated secondary antibody (1:3000) at RT, triplicate washes were followed with TBS-T, and developed for visualization using an ECL detection kit by Luminescent Image Analyzer, LAS-3000 (Fuji, Tokyo, Japan).

2.6. Statistical Analysis

Statistical analyses were performed on data collected in triplicate for all the experiments. All quantitative results are presented as means \pm standard deviations (SD). Statistical analyses were performed using Prism 5 software (GraphPad Software, San Diego, CA, USA), and statistical significance was determined by one-way ANOVA followed by Dunnett's test.

3. Results and Discussion

3.1. Identification of compounds from *Lindera obtusiloba*

Seven compounds were isolated from the 50% EtOH extract of *L. obtusiloba* Blume. The EA fractions are composed of seven lignans (**1-7**). Structure determination was performed using spectroscopic data, including ¹H NMR, ¹³C NMR, ¹H-¹H COSY, HMBC, HMQC, HRESIMS, and polarimetry. Comparing the spectroscopic data of the isolated compounds to published literature reports, the known compounds were identified as episesamin (**1**) [11], 2-(1,3-Benzodioxol-5-yl)tetrahydro-4-[(4-hydroxy-3-methoxyphenyl)methyl]-3-furanmethanol (**3**) [21], (+)-syringaresinol (**3**) [4], (7'S,8'R,8R)-lyoniresinol-9-O-(E)-feruloyl ester (**4**) [23], (-)-(2R,3R)-1-O-feruloyl-8,8'-bisdihydrosiringenin (**5**) [24], (-)-Lyoniresinol (**6**) [23] and Schizandriside (**7**) [25].

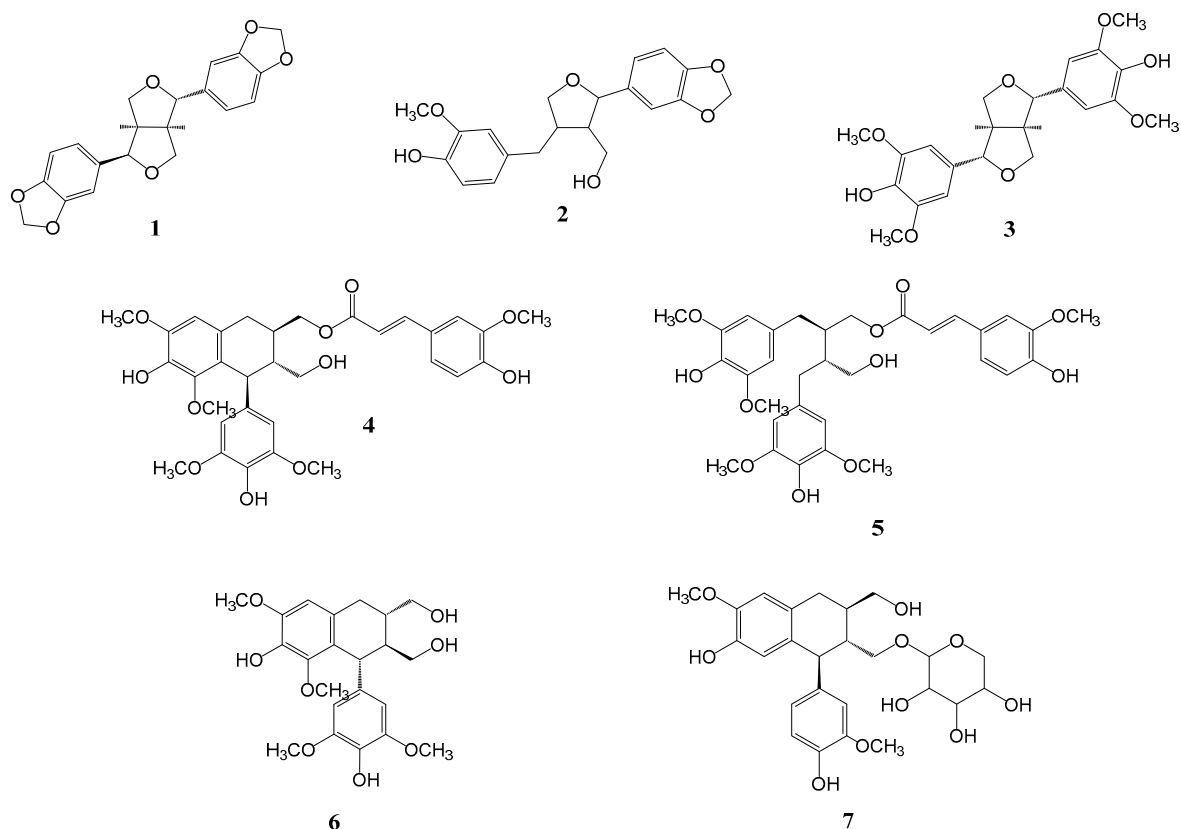


Figure 1. Structure of isolated compounds 1-7 of *L. obtusiloba*.

3.2. *L. Obtusiloba* Blume extract and fractions inhibit IL-6-induced pSTAT3 luciferase activity.

To identify IL-6/STAT3 inhibitors, IL-6-induced STAT3 activity was confirmed by luciferase assay using Hep3B cells stably expressing pSTAT3-luc. The cells were stimulated with IL-6 (10 ng/ml) for 12 h in the presence or absence of the EtOH extract or the fourteen fractions (n-hexane, chloroform, ethyl acetate, butanol, water, EA fraction 1~10). Treatment of Hep3B cells with IL-6 alone for 12 h led to an approximately 17-fold increase in pSTAT3-Luc activity, an increase that was substantially and dose-dependently inhibited by pre-treatment with the extract and fractions for 1 h. The EA-6 fraction was found to be the most effective for inhibiting IL-6-induced pSTAT3-Luc activation, followed by the EA-7 fraction and hexane layer. The MTT assay was employed to evaluate cytotoxicity at the tested concentrations. The EA7 and 10 $\mu\text{g/ml}$ EA6 fractions were found to be toxic, while all other concentrations were found to be cytotoxic. Except for the 100 $\mu\text{g/ml}$ EA concentration, hexane, EA7 and the rest of the EA6 concentrations exhibited over 80% cell survival, suggesting that the inhibitory effects of these substances on IL-6-induced STAT3 activation were not related to cytotoxicity.

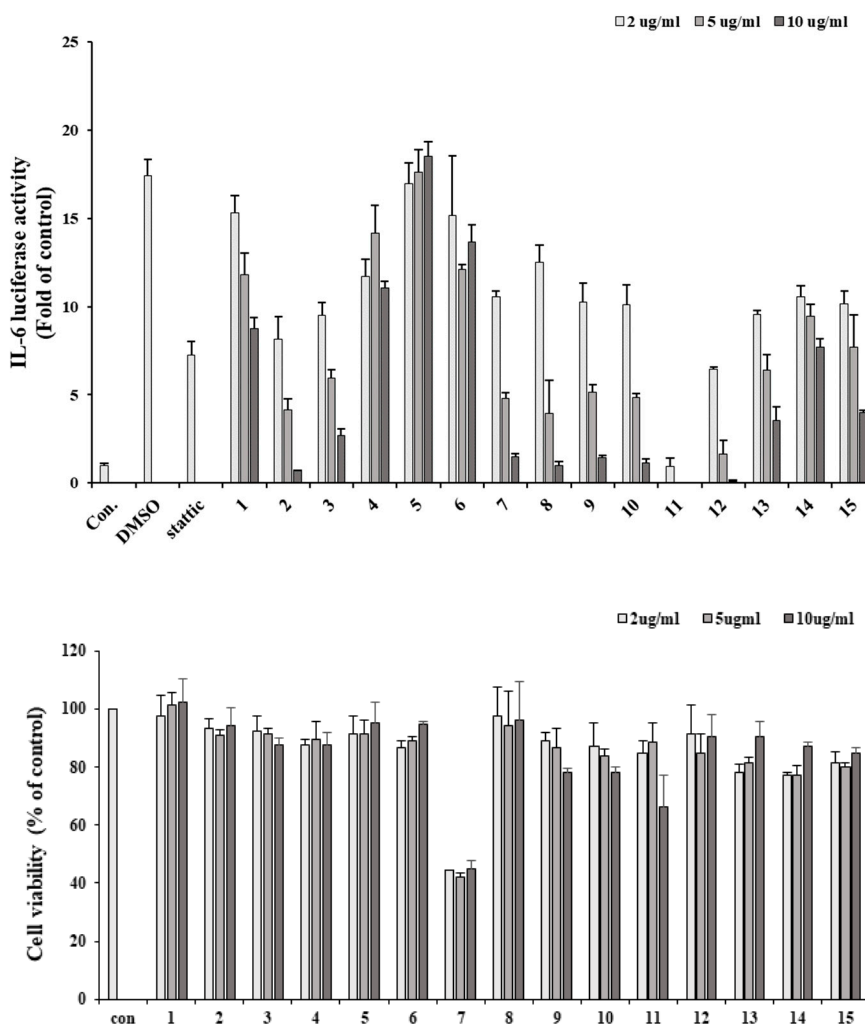


Figure 2. IL-6 induced STAT3 inhibitory effect of *L.obtusiloba* extract and fractions were evaluated using a luciferase assay in Hep3B cells (1). The viability of Hep3B cells after treatment with *L.obtusiloba* extract and fractions. 1: 50% EtOH extract, 2: Hexane fraction, 3: Ethyl acetate, 4: Butanol, 5: water, 6 - 15: EA fraction 1 – 10.

3.3. Inhibitory effects of isolated compounds on IL-6 induced pSTAT3 luciferase activity

All isolated compounds were measured for their inhibitory effect on IL-6-induced pSTAT3 luciferase activity in Hep3B cells. Additionally, an MTT assay was employed to evaluate cytotoxicity at the tested concentrations (data not shown), and the results indicated that the observed bioactivities were not due to cellular cytotoxic effects. Among the tested compounds, compound 5 showed the most significant inhibitory effects with an IC_{50} value of 10.83 μ M, which was compared with static (a positive control with an IC_{50} value of 0.27 μ M). Additionally, compound 1 exhibited high inhibitory effects with an IC_{50} value of 14.3 μ M, and compound 4 exhibited a slight inhibitory effect with an IC_{50} value of 40.39 μ M. Considering these results with respect to preliminary structural requirements for activity, two partial structures responsible for the bioactivity could be suggested as follows: a feruloyl moiety and a 1,4-diphenylbutane moiety. Based on these bioassay results, we hypothesized that compound 1 and 5 could be promising IL-6/STAT3 inhibitors.

Table 1. Inhibitory effect of compounds 1-7 on IL-6/STAT3 activation.

| compounds | IC ₅₀ (μ M) |
|----------------------|-----------------------------|
| 1 | 14.3 \pm 2.67 |
| 2 | >50 |
| 3 | >50 |
| 4 | 40.39 \pm 3.71 |
| 5 | 10.83 \pm 2.40 |
| 6 | >50 |
| 7 | >50 |
| stattic ^a | 0.27 \pm 0.03 |

Data are expressed as the IC₅₀ values of three independent experiments (n=3). ^a Stattic was used as the positive control.

3.4. Inhibitory effects of active compounds on IL-6 induced gene expressions

Next, we investigated whether the IL-6-induced pSTAT3 luciferase inhibitory effects of compounds affect pSTAT3 induced gene expressions. To confirm that, gene expressions of CRP, IL-1 β and SOCS3 were analyzed using quantitative real time PCR. The gene expressions were significantly downregulated 30 μ M of compound 1 and 30 and 60 μ M of compound 5 treatment (Figure 3).

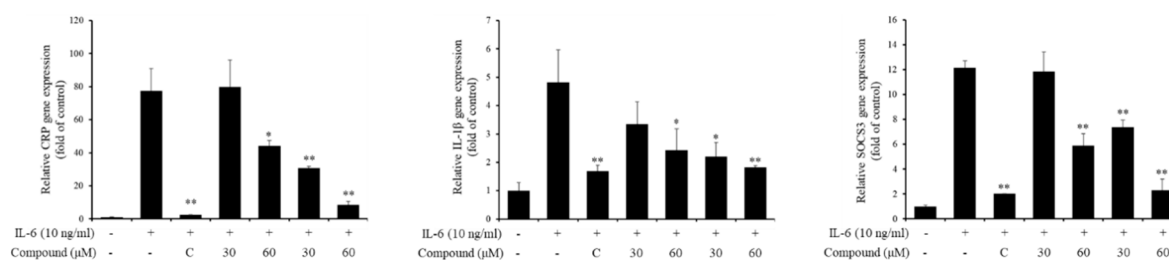


Figure 3. Effects of compounds 1 and 5 on the mRNA expression of IL-6-induced gene expressions. Hep3B cells were pretreated with 1 and 5 at 30 and 60 μ M for 1 h and induced with IL-6 (10 ng/mL) for 5 h. The gene expressions were analyzed using real-time PCR. C, 20 μ M of cirsiolol. * p <0.05, ** p <0.01 compared with the only IL-6 treated group. Values are expressed as the means \pm S.D. of three individual experiments. * p < 0.05 and ** p < 0.01 versus the only- IL-6-treated control group obtained through one-way ANOVA followed by Dunnett's test.

3.5. Effect of compound 1 and 5 on IL-6/STAT3 signaling molecules

To determine inhibitory mechanism of pSTAT3-induced gene, pSTAT3 expressions of Hep3B cells were investigated using immunofluorescence staining. The results showed that the compounds downregulated pSTAT3 nuclear translocation and pSTAT3 expression (Figure 4). Furthermore, western blot analysis of JAK2 and STAT3, which are IL-6 signaling molecules, the compound treatment decreased phosphorylations of JAK2 and STAT3 (Figure 5). These results indicate that the compounds regulate IL-6/STAT3 signaling through JAK2.

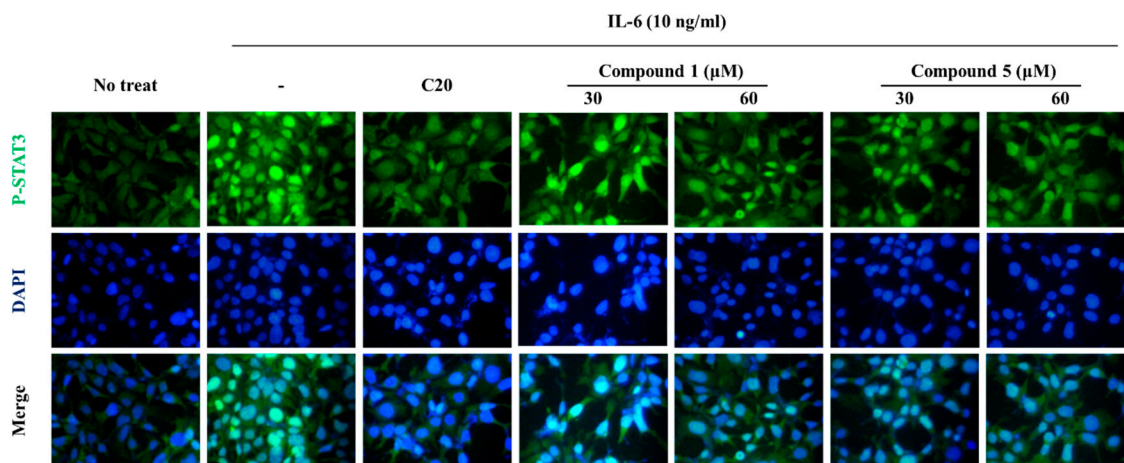


Figure 4. Effects of compound 1 and 5 on IL-6-induced p-STAT3 expression in Hep3B cells. Representative green fluorescence microscopy images indicating pSTAT3 stained by Alexa 488 and blue fluorescence microscopy images indicating the nucleus stained by DAPI. The Hep3B cells were treated with compounds 1 and 5 for 1 h and stimulated with 10 ng/ml IL-6 for 30 min. C20, 20 μ M of cirsiolol.

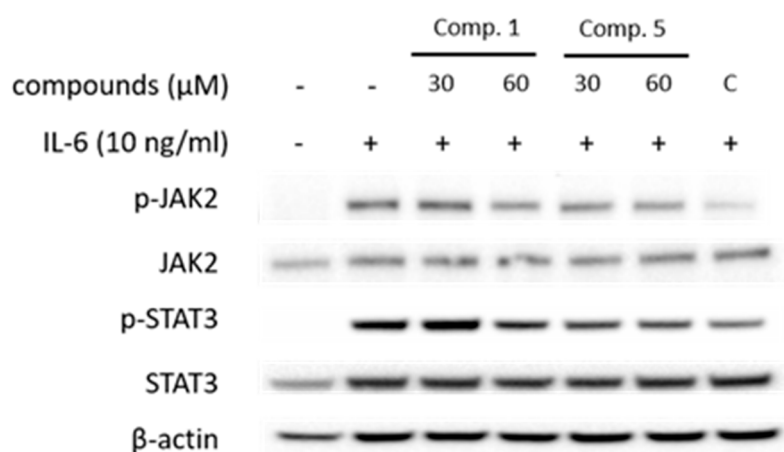


Figure 5. Effects of compounds 1 and 5 on the IL-6-induced phosphorylation of JAK2 and STAT3 in U266 cells. Cells were pretreated with compound 1 and 5 at 30 and 60 μ M for 1 h and treated with IL-6 (10 ng/ml) for 20 min. The p-STAT3 and p-JAK2 proteins were detected by Western blot analysis. The total nonphosphorylated proteins served as a loading control for the phosphorylated protein.

4. Conclusions

The stems of *Lindera obtusiloba* Blume are known to have inhibitory effects on various inflammatory responses such as neuroprotective activity and anti-allergic activity [13,15]. Based on this, compounds with potential as a promising inflammatory response inhibitor from the stems of *Lindera obtusiloba* have been reported. Previous physiochemical studies have represented that it consists of secondary metabolites such as lignan, neolignan, flavonoids, and butanolide [3–5]. In particular, compounds of the lignan family, such as xanthoxyol, syringaresinol, and linderin A, have been reported to have inhibitory activity against various inflammatory diseases [15]. In this study, compounds with IL-6-induced STAT3 inhibitory activities from the stems of *Lindera obtusiloba* Blume are investigated. There are seven types of compounds isolated from the 50% ethanol extract of *Lindera obtusiloba* Blume stem, and the structures of isolated compounds were identified using NMR and MS. The isolated compounds were mainly compounds of lignan family. These have structural features linked through C8-C8' linkage. Most lignans represent physiologically important functions for plant

defense and human health. Lignans are grouped according to functional groups such as furofuran, tetrahydrofurans, dibenzylbutanes and aryl naphthalenes [26,27].

IL-6 is a major cytokine involved in the inflammatory response and is a key upstream mediator of STAT3 [17]. IL-6 signaling is provoked by binding IL-6 to IL-6 receptor (IL-6R) complexes, which are related with IL-6, IL-6Ra, and gp130 receptor chains, and its activation result in the JAK2/STAT3 and MAPK signaling pathways [18,19]. The IL-6-induced JAK2/STAT3 signaling pathway plays a positive role in inflammation and neoplasia. The regulation of IL-6 is a useful method to inhibit the inflammatory response by regulating the phosphorylation of JAK2 and STAT3. All the isolated compounds (1-7) were evaluated for their IL-6-induced STAT3 inhibitory effects in Hep3B cells using a luciferase reporter assay. Additionally, we investigated whether compounds could inhibit the phosphorylation of STAT3 and JAK2.

In conclusion, the isolated compounds are identified for lignan family having furofuran and naphthalene functional groups. All the isolated compounds (1-7) were evaluated for their IL-6-induced STAT3 inhibitory effects in Hep3B cells using a luciferase reporter assay. Of the isolates, compounds 1 and 5 showed strong inhibitory effects on IL-6-stimulated STAT3 activation. These results can provide valuable biochemical information for the use of *L. obtusiloba* as a pharmaceutical material, and the bioactive compounds obtained from this plant may be promising candidates for the treatment of IL-6-mediated STAT3 disease. Further studies will be needed to elucidate the precise mechanism of these materials on the up- or downstream IL-6 signaling pathways, and their therapeutic efficacies as potent IL-6 inhibitors will be investigated *in vivo*, such as in arthritis or ovariectomized animal models.

Acknowledgments: This work was supported by Korea Institute of Planning and Evaluation for Technology in Food, Agriculture and Forestry (IPET) through Crop Viruses and Pests Response Industry Technology Development Program, funded by Ministry of Agriculture, Food and Rural Affairs (MAFRA)(120087-5) and a grant from the KRIBB Research Initiative Program (KGM5242113).

References

1. Haque, M.E.; Azam, S.; Balakrishnan, R.; Akther, M.; Kim, I.S. Therapeutic potential of *Lindera obtusiloba*: Focus on antioxidative and pharmacological properties. *Plants*. **2020**, *9*, 1765.
2. Hong, C.O.; Rhee, C.H.; Won, N.H.; Choi, H.D.; Lee, K.W. Protective effect of 70% ethanolic extract of *Lindera obtusiloba* Blume on tert-butyl hydroperoxide-induced oxidative hepatotoxicity in rats. *Food and chemical toxicology*. **2013**, *53*, 214-220.
3. Park, J.C.; Yu, Y.B.; Lee, J.H. Isolation and structure elucidation of flavonoid glycosides from *Lindera Obtusiloba* BL. *J Korean Soc Food Nutr*. **1996**, *25.1*, 76-79.
4. Kwon, H.C.; Choi, S.U.; Lee, J.O.; Kwon, H.C.; Choi, S.U.; Lee, J.O.; Bae, K.H.; Zee, O.P. Lee, K.R. Two New Lignan from *Lindera obtusiloba* blume. *Arch Pharm Res*. **1999**, *22*, 417-422.
5. Kwon, H.C.; Baek, N.I.; Choi, S.U.; Lee, K.R. New cytotoxic butanolides from *Lindera obtusiloba* BLUME. *Chemical & Pharmaceutical Bulletin*. **2000**, *48.5*, 614-616.
6. Suh, W.M.; Park, S.B.; Lee, S.; Kim, H.H.; Suk, K.; Son, J.H.; Kwon, T.K.; et al. Suppression of mast-cell-mediated allergic inflammation by *Lindera obtusiloba*. *Experimental Biology and Medicine*. **2011**, *236.2*, 240-246.
7. Park, K.J.; Park, S.H.; Kim, J.K. Anti-wrinkle activity of *Lindera obtusiloba* extract. *J Soc Cosmet Sci Korea*. **2009**, *35*, 317-323.
8. Bang, C.Y.; Won, E.K.; Park, K.W.; Lee, G.W.; Choung, S.Y. Antioxidant activities and whitening effect from *Lindera obtusiloba* BL. Extract. *Yakhak Hoeji*. **2008**, *52.5*, 355-360.
9. Kim, J.H.; Lee, J.; Kang, S.; Moon, H.; Chung, K.H.; Kim, K.R. Antiplatelet and antithrombotic effects of the extract of *Lindera obtusiloba* leaves. *Biomol Ther*, **2016**, *24.6*, 659-664.
10. Lee, J.O.; Oak, M.H.; Jung, S.H.; Park, D.H.; Auger, C. An ethanolic extract of *Lindera obtusiloba* stems causes NO-mediated endothelium dependent relaxations in rat aortic rings and prevents angiotensin II-induced hypertension and endothelial dysfunction in rats. *Naunyn Schmiedebergs Arch Pharmacol*. **2011**, *383*, 635-645.
11. Seo, K.H.; Baek, M.Y.; Lee, D.Y.; Cho, J.G. Isolation of Flavonoids and Lignans from the Stem Wood of *Lindera Obtusiloba* Blume. *J Appl Biol Chem*. **2011**, *54.3*, 178-183.
12. Kwon, D.J.; Kim, J.K.; Bae, Y.S. Essential oils from leaves and twigs of *Lindera obtusiloba*. *J Korean For Soc*. **2007**, *96.1*, 65-69.
13. Lee, K.Y.; Kim, S.H.; Jeong, E.J.; Park, J.H.; Kim, S.H. Kim, Y.C. Sung, S.H. New Secoisolariciresinol Derivatives from *Lindera obtusiloba* Stems and Their Neuroprotective Activities. *Planta Med*. **2010**, *76.03*, 294-297.

14. Ruehl, M.; Erben, U.; Kim, K.; Freise, C.; Dagdelen, T.; Eisele, S.; Trowitzsch-Kienast, W.; Zeitz, M.; Jia, J.; Stickel, F.; Somasundaram, R. Extracts of *Lindera obtusiloba* induce antifibrotic effects in hepatic stellate cells via suppression of a TGF- β -mediated profibrotic gene expression pattern. *J Nutr Biochem.* **2009**, *20*, 597–606.
15. Choi, H.G.; Choi, Y.H.; Kim, J.H.; Kim, H.H.; Kim, S.H.; Kim, J.A. A new neolignan and lignans from the stems of *Lindera obtusiloba* Blume and their anti-allergic inflammatory effects. *Arch Pharm Res.* **2014**, *37*, 467–472.
16. Freise, C.; Erben, U.; Neuman, U.; Kim, K.; Zeitz, M.; Somasundaram, R.; Ruehl, M. An active extract of *Lindera obtusiloba* inhibits adipogenesis via sustained Wnt signaling and exerts anti-inflammatory effects in the 3T3-L1 preadipocytes. *J Nutr Biochem.* **2011**, *21*, 1170–1177.
17. Mark, D.T.; Belinda, N.; Tara, H.; Daniel, J.P. Cytokines and chemokines: At the crossroads of cell signalling and inflammatory disease. *Biochimica et Biophysica Acta.* **2014**, *1843*, 2563–2582.
18. Kumari, N.; Dwarakanath, B.S.; Das, A.; Bhatt, A.N. Role of interleukin-6 in cancer progression and therapeutic resistance. *Tumour Biol.* **2016**, *37*, 11553–11572.
19. Hunter, C.A.; Jones, S.A. IL-6 as a keystone cytokine in health and disease. *Nat Immunol.* **2015**, *16*, 448–457.
20. Mihara, M.; Hashizume, M.; Yoshida, H.; Suzuki, M.; Shiina, M. IL-6/IL-6 receptor system and its role in physiological and pathological conditions. *Clinical science.* **2012**, *122*, 143–159.
21. Jang, H.J.; Lim, H.J.; Park, E.J.; Lee, S.J.; Lee, S.; Lee, S.W.; Rho, M.C. STAT3-inhibitory activity of sesquiterpenoids and diterpenoids from *Curcuma phaeocaulis*. *Bioorganic Chemistry.* **2019**, *93*, 103267.
22. Lee, S.J.; Jang, H.J.; Kim, Y.; Oh, H.M.; Lee, S.; Jung, K.; Rho, M.C. Inhibitory effects of IL-6-induced STAT3 activation of bio-active compounds derived from *Salvia plebeia* R. Br. *Process Biochemistry.* **2016**, *51*, 2222–2229.
23. Liu, Z.; Saarin, N.M.; Thompson, L.U. Sesamin is one of the major precursors of mammalian lignans in sesame seed (*Sesamum indicum*) as observed in vitro and in rats. *The Journal of Nutrition.* **2006**, *136*, 906–912.
24. Chang, C.M.; Chen, T.H.; Huang, Y.H.; Lin, J.J. Cytotoxic lignan ester from *cinnamomum osmophloeum*. *Planta Med.* **2009**, *76*, 613–619.
25. Sadhu, S.K.; Khatun, A.; Phattanawasin, P.; Ohtsuki, T.; Ishibashi, M. Lignan glycosides and flavonoids from *Saraca asoca* with antioxidant activity. *J Nat Med.* **2007**, *61*, 480–482.
26. Rahman, M.A.; Katayama, T.; Suzuki, T.; Nakagawa, T. Stereochemistry and biosynthesis of (+)-lyoniresinol, a syringyl tetrahydronaphthalene lignan in *Lyonia ovalifolia* var. *elliptica* I: isolation and stereochemistry of syringyl lignans and predicted precursors to (+)-lyoniresinol from wood. *Journal of wood science.* **2007**, *53*, 161–167.
27. Chen, T.H.; Huang, Y.H.; Lin, J.J.; Liao, B.C.; Wang, S.Y.; Wu, Y.C.; Jong, T.T. Cytotoxic lignan esters from *Cinnamomum osmophloeum*, *Planta medica.* **2010**, *76*, 613–619.

Disclaimer/Publisher's Note: The statements, opinions and data contained in all publications are solely those of the individual author(s) and contributor(s) and not of MDPI and/or the editor(s). MDPI and/or the editor(s) disclaim responsibility for any injury to people or property resulting from any ideas, methods, instructions or products referred to in the content.